Hybrid forming process of AA 6108 T4 thin sheets: modelling by neural network solutions

M Barletta[1], A Gisario[2], and S Guarino[1]*
[1]Department of Mechanical Engineering, University of Rome, Rome, Italy
[2]Department of Mechanics and Aeronautics, La Sapienza University of Rome, Rome, Italy

The manuscript was received on 7 May 2008 and was accepted after revision for publication on 17 September 2008.

DOI: 10.1243/09544054JEM1218

Abstract: The highly non-linear deformation processes occurring in most dynamic sheet metal forming operations cause large amounts of elastic strain energy to be stored in the formed material and massive related springback phenomena. Therefore, this paper investigates how effective a laser source is in reducing the extent of springback in mechanical contact forming operations.

The hybrid forming process investigated was composed of using a high-power diode laser to induce local heating of mechanically bent AA 6108 T4 thin sheets in order to minimize the extent of the springback. In particular, experiments were carried out to assess the influence of the leading process parameters such as laser source power, scan speed, and starting elastic deformation of the mechanically bent sheets. It was found that the trends in the experimental response of residual deflection were always consistent with the operating parameters.

Artificial intelligence techniques were then used to model the hybrid forming process. The extent of the springback in the hybrid forming process of AA 6108 T4 thin sheets was predicted by using different neural network models and training algorithms. Lastly, the reliability of the best neural network solutions was checked by comparing these solutions with experimental results and by developing an *ad hoc* first approximation technical model.

Keywords: aluminium alloy, bending process, diode laser, neural network model

1 INTRODUCTION

Sheet metal forming is an operation in which a material is plastically formed into a desired shape. One of the most widely used sheet metal forming processes is bending. This operation is employed in the automotive and aerospace industries in addition to several other industrial sectors [**1**]. Predictability and reproducibility of sheet metal forming processes are mainly derived from the variations in blank dimensions, material properties, and environmental conditions. However, it is the springback phenomenon that causes most deviation of the end-product from the designed shape and underlies most of the drawbacks in assembly operations. Consequently, springback is a critical issue that must be taken into consideration when designing forming dies [**2**, **3**]. In most dynamic sheet metal forming operations, the highly non-linear deformation processes generate a large amount of elastic strain energy in the bent material. This elastic strain energy is stored in the material during the contact with the die and subsequently released when the contact pressure ceases. Springback phenomena are strictly related to this release of energy and cause uncontrolled geometrical alterations to the part being bent [**3–6**]. Therefore, the final shape of the end-product not only depends on the geometry of the dies but also on the amount of elastic energy stored in the deformed material after the load is removed. At the same time, the amount of elastic energy stored in the deformed material depends on many parameters but particularly on material properties, contact conditions, and interfacial loads. Consequently, predicting the extent of springback during forming is a very critical issue and

Corresponding author: Dipart di Ingegneria Meccanica, University of Rome, Tor Vergata, Via del Politecnico, 1-00133 Rome, Italy. email: stefano.guarino@uniroma2.it

thus designers and practitioners experience considerable difficulties designing a new die.

At the time of writing springback compensation was still essentially composed of empirical rules or straightforward analyses based on *trial-and-error* procedures, which are widely available for simple shapes on well-known materials. However, the increasing demand for new shapes and exotic materials requires extensive use of recursive optimization procedures, which inevitably results in significant increases in the overall manufacturing costs. Consequently, several sophisticated approaches to confronting the springback phenomena in metal sheet forming have been proposed in the literature. For example, Liu [**7**] was the first to propose a method of reducing springback. His method increases the restraining force in steps. During the forming cycle, Liu imposed a binder force path by using an *intermediate restraining* process to form complex shapes in a single operation. The variation of the binder force during the process provided a tensile load on the part being formed which significantly reduced springback. However, meticulous controls during the process were required, making this approach very sensitive to any variation in operating conditions and in material properties (especially the friction coefficient). In addition, this approach cannot eliminate springback when forming complicated profiles. Then 10 years later Sunseri *et al.* [**8**] developed a closed-loop algorithm for binder force control to make the forming process more robust and repeatable. Following this, Moon *et al.* [**9**] studied the effects of die and punch temperatures on springback phenomena. They found that the combination of a hot die and a cold punch could reduce springback up to 20 per cent compared to the conventional room temperature bending process. However, this approach has not become widespread yet because it increases costs and lowers process efficiency compared to the other forming techniques. More recently, the laser forming process has become quite important in many manufacturing sectors such as the automotive, microelectronics, and aerospace industries [**10–12**]. Laser forming does not need any external force, so springback may be negligible. Also, it can shape a complex surface and even produce very small parts or features. Moreover, several hard and brittle materials such as titanium alloy, nickel alloy, ceramics, etc., can be usefully processed. Unfortunately, compared to conventional forming technologies laser forming is a time-consuming and costly process. However, it is competitive as a support to conventional forming processes when springback phenomena need to be minimized.

Hybrid forming processes in which mechanical bending is assisted by laser or *vice versa* are recent innovations and so only a few studies are currently available in the literature [**13–15**]. Little understanding of the major phenomena involved in laser heating of the parts being bent, increased running and operating costs, as well as problematic process control and monitoring have all significantly restricted the widespread adoption of hybrid forming. Furthermore, the absence of analytical modelling techniques and related simulation tools results in the use of these innovative forming technologies being further restricted.

This is the context in which the present study investigates using a high-power diode laser to support the conventional mechanical contact forming process of AA 6108 T4 thin sheets to overcome the issues mentioned above. A laser source focused on critical areas during sheet forming operations should induce localized heating of the component, thus releasing most of the energy stored during the mechanical contact forming process thereby reduce springback. Consequently, several operating parameters such as laser power, scan speed, and preloading the part to be bent in the elastic range all influence the evolution of the hybrid forming process and its modelling, which form the subject of the results presented in this paper. In particular, the experimental analysis focuses on predicting the residual deflection of the part being bent after the release of the applied preload and following completion of the laser processing. Design of experiments (DOE) techniques were used to assist the experimental investigation. Consequently, the trends in the experimental response residual deflection were achieved by varying the setting of the process parameters. Analysis of variance (ANOVA) was also used to assess the *significance* of each operational parameter and evaluate the simple and interactive effects of the experimental factors investigated. Finally, artificial intelligence techniques were used to model the whole hybrid forming process. The springback phenomena of AA 6108 T4 thin sheets subject to the hybrid forming process was predicted by using different neural network models and training algorithms. This enabled the reliability of the best neural network solutions to be evaluated by comparing them with experimental results as well as with an *ad hoc* first approximation technical model.

2 EXPERIMENTS

2.1 Materials and equipment

As it is of commercial interest and widely used in several industrial markets, a laser-assisted forming process was carried out on an AA 6108 T4 aluminium alloy. $600 \times 600 \times 1.2\,\mathrm{mm}^3$ sheets (Pontecorvo Metalli, Roma, Italy) were cut into $150 \times 30 \times 1.2\,\mathrm{mm}^3$ samples

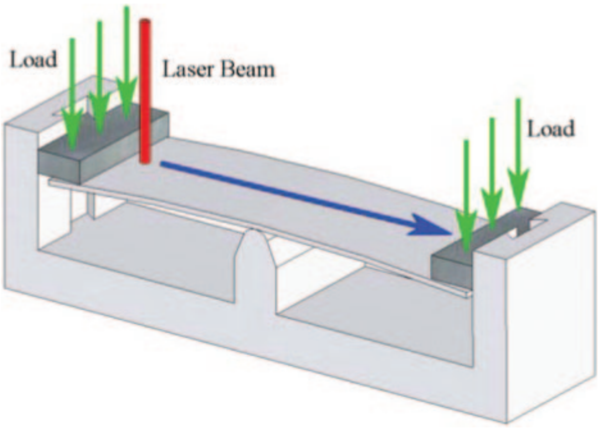

Fig. 1 Diagram of the inflexion system

by using an automatic standard blanking system (Dalcos model PXN 408). The closest geometrical tolerances (< 0.05 mm) and uniform starting surface conditions were ensured by thorough controls performed by a coordinate measuring machine (CMM Mitutoyo model CRISTA APEX C544). An ultrasound cleaning system (SOLTEC model Sonica 2200) was used to guarantee surface cleanliness of the samples before laser processing.

A mechanical contact bending process was performed using home-made automatic forming equipment (Fig. 1) composed of a three-point bending load system that, in strictly controlled conditions, induces a prescribed starting deflection in the elastic range on the aluminium sample.

Laser processing of the preloaded parts was performed using a high-power diode laser source (ROFIN-SINAR model DL 015), 1.5 kW maximum power, with a wavelength of 940 ± 10 nm and an elliptical spot, with dimensions of 1.9 mm along its major axis and 0.6 mm along its minor axis. Tests were performed by focusing the laser beam through a 63 mm focus lens. Furthermore, for reasons of protection and insulation, a flow of argon was continuously concentrated on the laser treated area during the bending tests.

2.2 Methodology

Hybrid forming tests measured the residual deflection of the preloaded aluminium sheets after laser processing and preload cessation. The basic idea is to preload the aluminium sheets at different ranges within their elastic limit. Then heating by laser should lower the elastic limit of the material and bring the pre-bent sheets within the plastic range, which reduces springback.

The following method was used to carry out the experiments.

Table 1 Experimental conditions

Experimental levels	Laser power (W)	Laser speed (mm/s)	Starting deflection (mm)
I	500	4	0.5
II	600	5	1
III	700	6	1.5
IV	800	7	2

Table 2 Amended experimental conditions

Experimental levels	Laser power (W)	Laser speed (mm/s)	Starting deflection (mm)
I	500	5	0.5
II	600	6	1
III	700	7	1.5
IV	–	–	2

1. The aluminium sheets were cleaned by using an ultrasound system to ensure the absorption coefficients of the sample surface under the laser source were the same (that is, the sheets had the same energy transfer efficiency).
2. Preloading the aluminium sheets to ensure a prescribed and well-defined starting deflection in the elastic range of the chosen material.
3. Laser processing along the median axis of the pre-bent aluminium sheets (i.e. laser source shown in the dark column and laser processing direction shown by the dark horizontal arrow as in Fig. 1) normal to the mechanical pre-bending direction.
4. Evaluation of the residual deflection (i.e. experimental response) of the pre-bent aluminium sheets after laser processing and removal of the applied load.

Table 1 summarizes the scheduling of the experimental tests. A full factorial experimental design was used that considered three operational parameters: laser power (range 500–800 W), laser scan speed (range 4–7 mm/s), and starting deflection (range 0.5–2 mm). The scheduled tests were repeated at least three times to ensure data repeatability and reproducibility. However, results achieved at too low a scan speed (4 mm/s) or too high a laser power (800 W) were affected by extensive melting phenomena on the surface of the sheets being treated, so the scheduling of the tests was changed to that reported in Table 2. Each test performed according to the new scheduling shown in Table 2 resulted in acceptable surface conditions on the bent aluminium sheets after laser processing so they could be used to estimate the actual value of the residual deflection.

2.3 Characterization tests and data modelling

The experimental response residual deflection was measured by using a non-contact CLA gauge (Taylor Hobson model CLI 2000). Ten profiles along the axial direction of the aluminium sheets with a step size of 0.5 mm were stored. The maximum deflection was evaluated for each profile and then averaged to produce a measurement of the mean residual inflexion of the formed sheets.

Analysis of mean (ANOM) was subsequently used to evaluate the variation of the experimental response residual deflection according to the operating parameters. After this, ANOVA was used to analyse the significance of the effects of each experimental factor and their effect on the experimental response residual deflection. Main effects and interaction plots were also drawn. A main effects plot (MEP) is a plot of the means at each level of a factor. A reference line at the grand mean of the response data is then drawn. A main effect occurs when the mean response changes across the levels of a factor. Accordingly, a MEP can be used to compare the relative strength of the effects across factors. An interactions plot (IP) is a plot of means for each level of a factor while the level of a second factor is held constant. IPs indicate the presence or absence of interaction. Interaction is present when the response at a factor level depends on the level(s) of other factors. Parallel lines in an IP indicate no interaction. The greater the departure of the lines from the parallel state, the higher the degree of interaction. To use an IP, data must be available from all combinations of levels.

Finally, based on statistical considerations, a first-approximation technical model was developed and its reliability verified by comparing it with the experimental results.

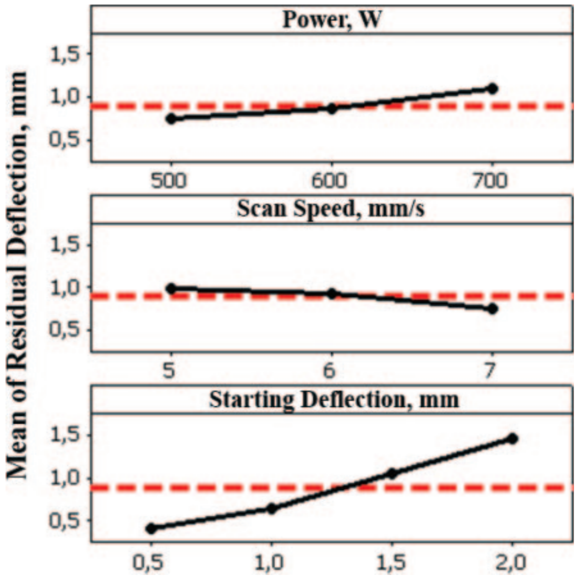

Fig. 2 MEP of the process parameters

3 RESULTS AND DISCUSSION

3.1 Analysis of process parameters

Figure 2 reports the MEP of the experimental response residual inflexion according to the experimental factors of laser power, laser scan speed, and starting deflection. Significant effects can be claimed for all the investigated experimental factors.

Laser power and scan speed together with the area of the irradiated zone define the energy input delivered to the AA 6108 T4 sheets during laser processing

$$F = \frac{Q \times \tau}{S} \tag{1}$$

where F is the energy input, Q is the laser power, τ is the interaction time (i.e. the ratio of the length of the path irradiated by the laser beam l to the laser scan speed v), S is the irradiated area (i.e. l multiplied by the major axis of the laser spot a). If the absorption of the sample surface, focus conditions, and the area of the laser-treated zone are all kept constant, then Q and v define the amount of energy supplied to the material being bent. Higher fluences delivered to the samples correspond to a higher laser power and lower scan speed and in both of these circumstances the residual deflection tends to assume the largest values, thus providing better compensation against springback phenomena. This is the best setting in the elastic range for the mechanically pre-bent part to keep its starting deflection. It stands to reason that in these process conditions the amount of energy transferred to the pre-bent sheet by laser irradiation is large enough to lower the elastic limit of the material, thus bringing it within the plastic range. This agrees with what was found in a previous study (by Geiger *et al.* [**14**]), and usefully reduces or even minimizes the related springback phenomena.

The ideal conditions in the experimental procedure were found to be a residual deflection equal to the starting deflection, which means no springback at all. However, this condition is unlikely to occur as an upper limit to the maximum value of the energy input deliverable to the sample being bent is represented by the surface status of the sample itself after laser processing. If the energy input assumes values larger than a threshold of approximately 36.8 J/mm^2, extensive melting of the aluminium surface takes place and significant geometrical alterations of the processed part can occur. Consequently, the sample being bent can be irremediably spoilt and is no longer of any use. Conversely, as soon as less energy input is delivered to the sample being bent, smaller values of the residual deflection are measured, thus making the difference between the preset starting deflection and that measured after release of the load and completion of laser processing larger. In these circumstances, the laser processing is progressively less effective as smaller amounts of energy are transferred to the sample being bent. Therefore, if the elastic limit of the material is not lowered too much, the pre-bent sheets are brought well within their plastic range. Consequently, springback is only slightly reduced, and in contrast to the case of larger energy inputs delivered to the samples, the springback is not minimized.

Although all the experimental factors investigated were found to produce significant main effects, starting deflection produces the largest main effect, that is, the largest variations in the experimental response residual deflection occur when the starting deflection experimental levels are changed. However, it is extremely important to evaluate the ability of laser processing to compensate for the springback phenomena by varying the preset starting deflection in a range wide enough for practical purposes (0.5–2 mm). In fact, the higher the preload (that is, the higher the preset starting deflection), the higher the amount of energy stored inside the sample being bent, which must subsequently be released once the preload action ceases and consequently the larger the extent of springback expected. However, a higher preload means that the pre-bent sheets are brought closer to the elastic limit of the material, that is, once heated they are brought closer to the plastic range. In contrast, a lower preload (that is, lower preset starting deflection) means a smaller amount of energy stored inside the sample being bent during the preload and so a smaller amount of energy is released after the removal of the applied load and so a smaller amount of springback can also be expected. However, a lower preload means that the pre-bent sheets are farther away from the elastic limit of the material, that is, farther away from the plastic range.

In the former case, the sheets are pre-bent to such an extent that the material is taken very close to its plastic range. Then even modest heating provided by laser irradiation further lowers the elastic limit of the material and takes the whole system well within the plastic range, thus concurrently minimizing the related springback phenomena. In the latter case, the material in the pre-bent sheet is far from being brought to its plastic range as the same laser irradiation is not enough to take the material within its plastic range, thus reducing but not minimizing springback. Despite the theoretical statements made above, the ratio between the residual deflection and the starting deflection (that is, normalized residual deflection) in Fig. 3 shows how the ability of laser processing to compensate the springback phenomena is invariate in relation to the preset starting deflection. Figure 3 reports all the data available, the mean of this data, and

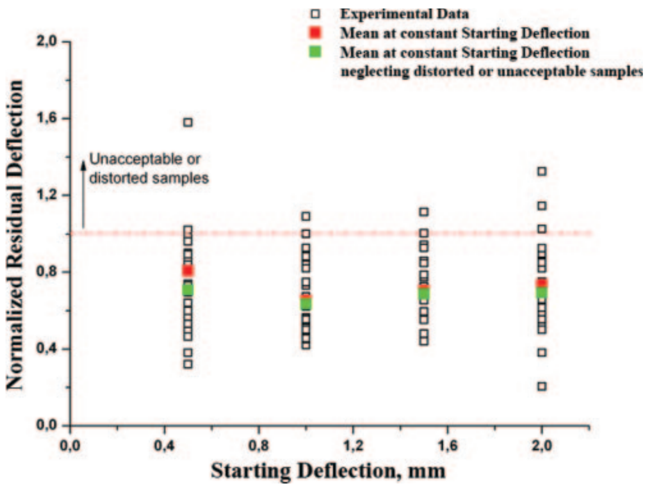

Fig. 3 Normalized residual deflection against starting deflection

their mean once anomalous data are neglected. In fact, some values of the normalized residual deflection are over one. This result is unacceptable in the light of the forming procedure employed. These inconsistencies are generally attributable to geometrical distortions induced in the samples being bent during laser processing because too much energy input is delivered on them (sheet bending as a result of the gravitational force acting on the almost molten material) or because of anomalies in the forming procedure that compromise the final result. However, mean values and the respective ranges in Fig. 3, once anomalous experimental data have been disregarded, are nearly the same whatever the preset starting deflection value, which confirms the proposed hybrid forming procedure has the same effect on the large operational ranges of starting deflection investigated. Consequently, no matter what the extent of springback to be compensated within the range investigated even at different preset starting deflection, laser processing always has the same effect on the pre-bent sheets. Normalized residual deflection of approximately 0.7 can be claimed throughout the range investigated, which means that only 30 per cent of the expected springback phenomena cannot be balanced properly. Therefore, the proposed hybrid forming system performs quite well on samples pre-bent in a broad range of elastic deformation.

3.2 ANOVA and technical model

ANOVA was then used to establish the *significance* of each experimental factor investigated and their interactions. The results of the ANOVA together with Fisher's factor F and contribution percentages Π are reported in Table 3. The analysis confirms that all the experimental factors influence the experimental response residual deflection. The most influential

Table 3 Results of the ANOVA analysis

Source	Degrees of freedom	Sum of squares	Mean-square	F	P
A - Laser power, W	2	2.255 09	1.127 54	22.41	8.329 393
B - Scan speed, mm/s	2	1.103 71	0.551 86	10.97	4.076 66
C - Starting deflection, mm	3	17.664 50	5.888 17	117.01	65.245 54
Interaction *AB*	4	0.382 31	0.095 58	1.90	1.412 099
Interaction *AC*	6	0.678 60	0.113 10	2.25	2.506 475
Interaction *BC*	6	0.666 31	0.111 05	2.21	2.461 081
Interaction *ABC*	12	0.700 08	0.058 34	1.16	2.585 813
Error	72	3.623 29	0.050 32	–	13.382 97
Total	107	27.073 88			

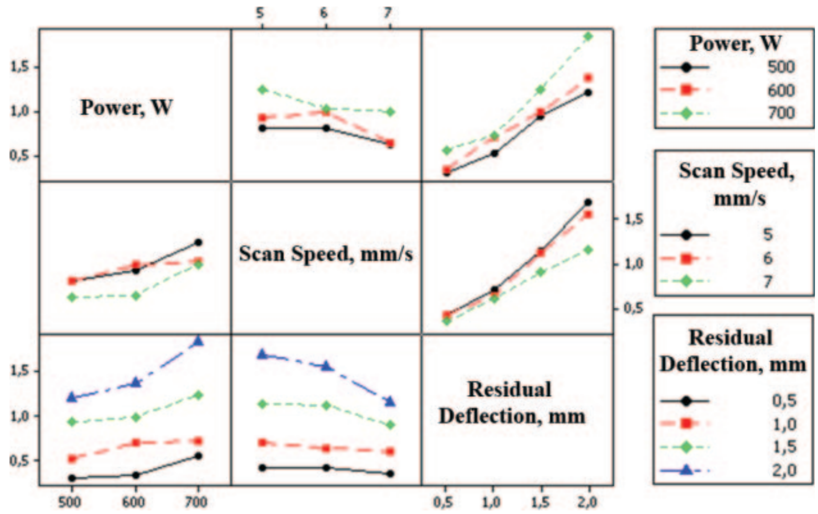

Fig. 4 IP for analysis of process parameters

experimental factor was found to be the starting deflection which had a Fisher's value of 117 ($F_{2,72,0.05}$ tabulated of 3.1 ([**16**])) as well as a contribution percentage Π of more than 65 per cent. The experimental factors of laser power (calculated value of the Fisher's factor of about 22.4) and scan speed (calculated Fisher's factor of approximately 10.9) exhibit Fisher's factors well above their respective calculated values and, therefore, they both influence the experimental response residual deflection. The percentage contribution is approximately 8.32 and 4.07 per cent for the experimental factors of laser power and scan speed respectively. These values are lower than in the case of the starting deflection, but they are large enough for practical purposes.

ANOVA reveals the presence of interactions with no *significance*. In fact, the Fisher's factors calculated for the interactions *AB*, *AC*, *BC*, and *ABC* reported in Table 3 are lower than the corresponding theoretical value ($F_{4,72,0.05}$ calculated value of 2.5, $F_{6,72,0.05}$ calculated value of 2.2 and $F_{12,72,0.05}$ calculated value of 1.9, respectively). Furthermore, their overall percentage contribution is less than 10 per cent, a result confirmed by the interactions plot in Fig. 4. It is well known that IP can be used to evaluate the impact that changing one experimental factor has on the other factors. A loss of parallelism in trends indicates interactions between the operational parameters and the presence of an interaction can magnify or diminish main effects. Consequently, evaluating the interactions can be very important [**16**]. In the present case, it is worth noting that because the trend lines run almost parallel, there are no particular interaction effects between the operating parameters investigated and the experimental response residual deflection.

The error values listed in Table 3 confirm the reliability of the experimental analysis. A percentage contribution due to error of approximately 13 per cent was found. This is largely acceptable in the light of the experimental plan developed, which is typically affected by non-negligible alterations and unpredictable deviations, which can be reflected in the goodness of the analysis [**13**].

Figure 5 displays the results of the analysis of the residuals. Normal probability plots show the residuals are mainly arranged in a straight line, with some departures from normality. The graph of the residuals against the fitted values shows that the residuals are

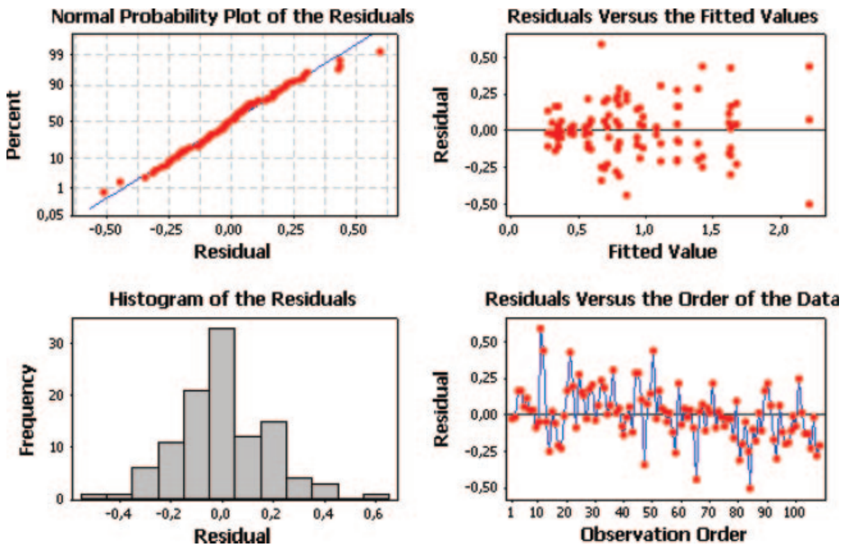

Fig. 5 Residuals plot: analysis of process parameters

Table 4 Results obtained using various modelling approaches

		MLP			GFF-MLP			RBF		
	Regression	Train	CV	Test	Train	CV	Test	Train	CV	Test
MSE	0.009	0.012	0.002	0.006	0.006	0.004	0.016	0.048	0.000	0.012
Mean absolute error	0.050	0.072	0.032	0.047	0.065	0.042	0.062	0.093	0.016	0.073
Minimum absolute error	0.000	0.001	0.006	0.000	0.011	0.007	0.000	0.002	0.002	0.001
Maximum absolute error	0.349	0.408	0.116	0.244	0.198	0.186	0.768	0.880	0.050	0.309
R	0.872	0.906	0.920	0.935	0.519	0.853	0.657	0.409	0.916	0.444

randomly distributed around zero. The histogram of the residuals also shows a Gaussian trend. The plot of residuals in the order of the corresponding observations fluctuates around the centre line in a random pattern, with no evidence of correlation between error terms. All of these aspects are evidence that the experimental plan is not affected by non-random or systematic error, thus providing further confirmation that the experimental data is reliable.

An ordinary least square regression model was built using the ANOVA results. Only the basic experimental factors have been accounted for as the influence of the interactions on the experimental response residual deflection is negligible.

Given that the residual deflection is i_r and the starting inflexion is i_s, the regression equation can be written as follows

$$i_r = k + \alpha Q + \beta v + \gamma i_s \tag{2}$$

Multiple regression of the experimental data was used to calculate the four coefficients in equation (2)

$$i_r = -0.334 + 0.00173Q - 0.118v + 0.710i_s \tag{3}$$

Equation (3) represents an *ad hoc* first-approximation technical model suitable for prediction and simulation.

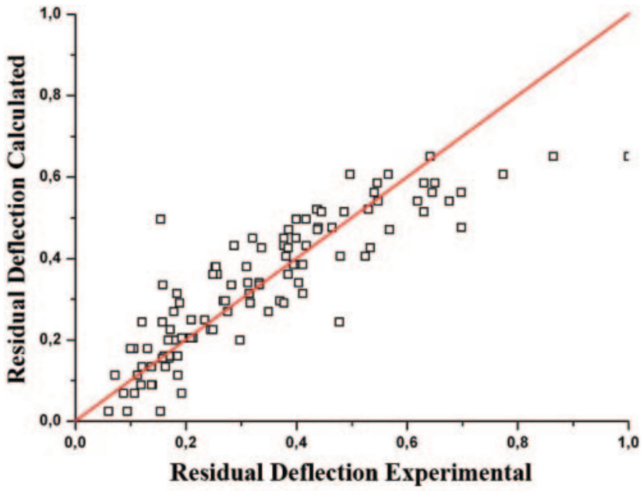

Fig. 6 Comparison of the experimental and predicted outputs for the regression model

Table 4 reports minimum, maximum, and mean absolute error, mean square error (MSE), and correlation factor *r*. An MSE of approximately 0.009 and correlation coefficient *r* of approximately 0.87 were found, thus confirming that the fit of the developed regression model is quite good. Figure 6 reports a good fit between the normalized experimental and calculated data. In order to develop more sophisticated models able to improve the fit of the experimental data and be suitable for more complex forming problems the neural network approach has been investigated and compared with the *ad hoc* technical model.

4 NEURAL NETWORKS

4.1 Neural network models

As springback is too difficult to calculate exactly by using experience and table checking, artificial neural networks (ANNs) are potentially useful in the modelling of the complex, non-linear, polytropic springback problem. ANNs supported by a genetic algorithm that are able to successfully solve the springback issue in typical U-shaped bending of thin metal sheets have already been proposed in the literature [**17**]. Therefore, artificial intelligence approaches were used to model the experimental results of the hybrid forming process of AA 6108 T4 thin sheets. The present case is characterized by simple shaping of the end-products, which is achieved using a combined forming process. Consequently, it is correct to consider it to be a complex forming problem.

The proposed hybrid forming process was modelled and simulated using three different neural network models: radial basic function (RBF), generalized feed forward (GFF), and multi-layer perceptron (MLP). Training of the MLP neural network was performed by using an adaptive learning rate backpropagation (BP) algorithm. A widely available commercial software (NeuroSolutions release 5.0 developed by NeuroDimension Incorporated) was chosen as the simulation tool.

4.2 Neural network set up

The three factors that have a significant effect on the experimental response residual inflexion were used as input processing elements (PEs) in the MLP, RBF, and GFF-MLPs neural network models, that is, laser

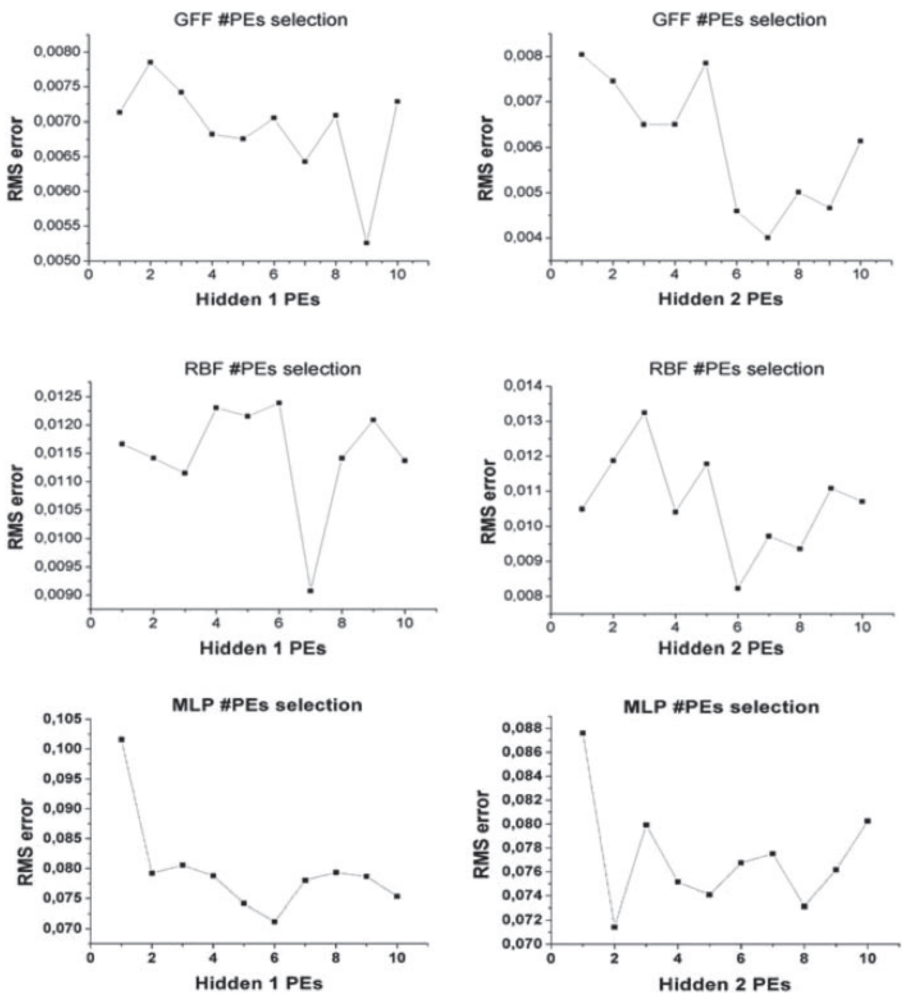

Fig. 7 RMS error as a function of PEs for the analysed neural network models

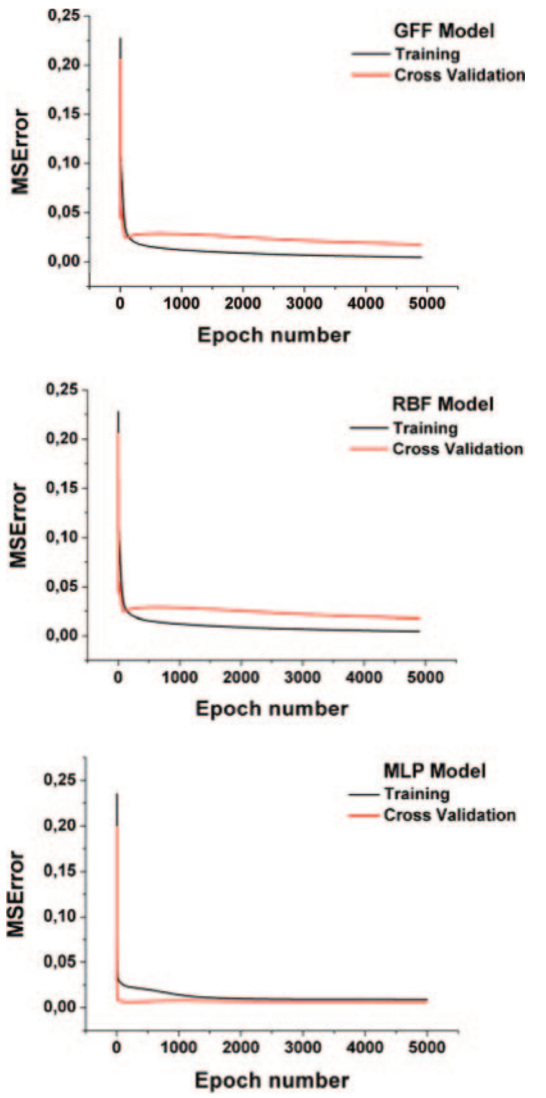

Fig. 8 RMS error as a function of the number of epochs for the considered neural network models

power, scan speed, and starting inflexion. The residual deflection was the only output estimated. A total of 108 samples (i.e. experimental data) were analysed. The available experimental data were shared according to the following percentages: 60 per cent as training, 15 per cent as cross-validation, and 25 per cent as testing. The learning rule was based on the momentum with step size being set at one and a momentum coefficient for the hidden layers being set at 0.7. The three chosen networks were then trained. In order to obtain a good indicator of the generalization level achieved by the networks, training was stopped when the MSE of the cross-validation set began to increase, this being a signal that the networks were becoming over-trained.

Different setups for the neural network models were examined to find the best solutions for predicting the experimental trends of the hybrid forming process. In particular, the use of single and double hidden layers was tested. Figure 7 displays the performance of the three neural networks employed. The effect on the RMSE of the number of PEs in the hidden layer is reported. The use of two hidden layers seems to guarantee the best results whatever the neural network model selected. Accordingly, the MLP network was set with five PEs for the first layer and three PEs for the second one, the RBF network was set with seven PEs for the first layer and six PEs for the second layer, and the GFF-MLP was set with nine PEs for the first layer and seven PEs for the second layer.

Figure 8 shows the RMSE trends according to the number of epochs for all the models chosen. The number of epochs for each neural network model was fixed at 5000. The MLP model had the lowest RMSE, followed by GFF-MLP, while RBF presented the highest RMSE.

4.3 Modelling of the experimental data

The experimental data for the hybrid forming process was modelled using the aforementioned neural network models. The capabilities of the developed models were checked by comparing the output with the available experimental data. Figure 9 is a comparison between the output calculated by the network (testing set) and the experimental results. The MLP trained with the BP algorithm was found to be the model with the best fit. Using this, the neural network solution obtains a correlation coefficient r very close to one for the training (0.906) and for the cross-validation set (0.920). It acheives a slightly higher value for the testing set (0.935). The MLP has a very low MSE and absolute error, as documented in Table 4. In particular, it displays a mean absolute error of just 0.047 for the testing set and an MSE of just 0.006. These values are lower than those calculated for the technical model. Therefore, the MLP guarantees a very accurate fit of the experimental data. The results obtained using the GFF and RBF models are not as good. They are characterized by lower correlation coefficients whichever training, cross-validation, or testing set is considered. Similarly, they are characterized by an MSE and mean absolute error, which are significantly higher than the corresponding values calculated for both the regression and MLP models.

The mean absolute error of approximately 4.7 per cent for the testing set of the MLP model is generally acceptable and it is definitely lower than the mean absolute error for the GFF and RBF, which are approximately 6.2 and 7.3 per cent, respectively. Fitting capabilities of the MLP model are therefore very good including when they are compared with data available in the literature. In fact, the literature

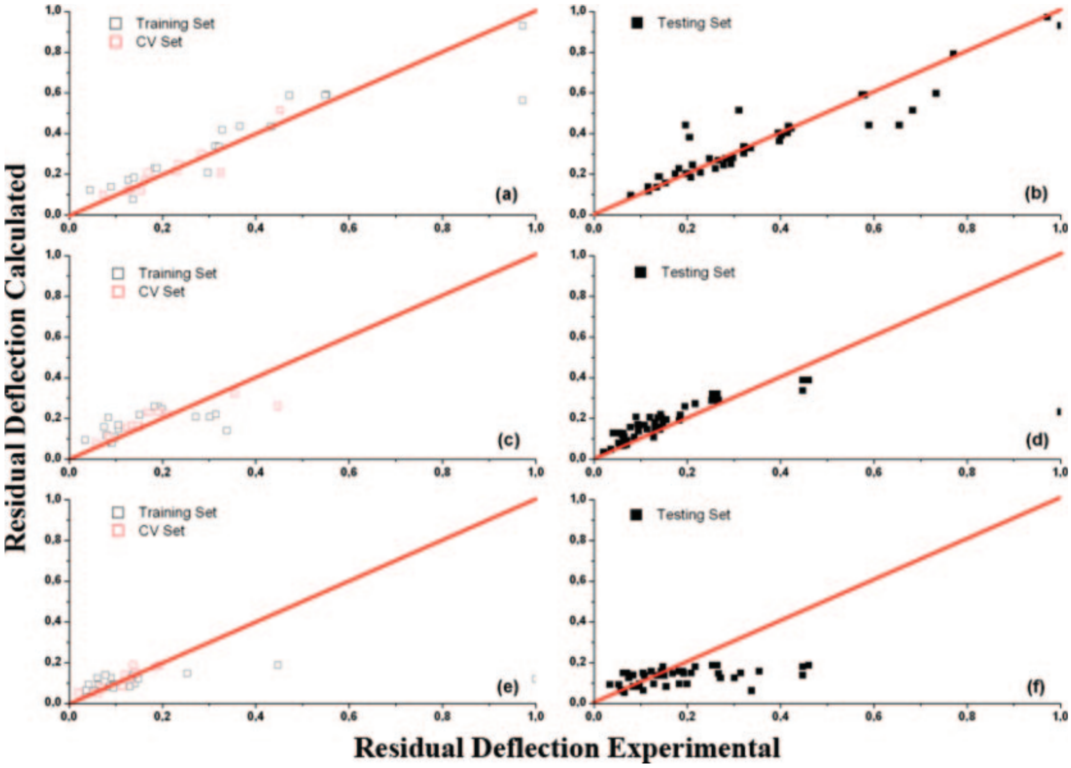

Fig. 9 Comparison of the experimental and predicted outputs for the considered neural network models

reports significantly higher errors (typically over 10 per cent and sometimes as large as 20 per cent) affecting the experimental procedures [**5–7**]. On the other hand, the ANOVA results reported in the previous section underline how, including the experiments in this paper, the variability of the hybrid forming process due to systematic errors and to the unpredictable factors can be significantly higher, which means the collected experimental data is very unreliable.

Finally, mean absolute errors greater than 5 per cent are quite common in all the applications in which neural network models are used, that is, in data prediction, in process modelling, and in simulation of most laser processing of metal and non-metal components [**18–20**]. This consideration further confirms the reliability of the developed MLP model and its suitability for analysing the hybrid forming process.

5 CONCLUSIONS

Hybrid forming experiments were carried out on AA 6108 T4 thin sheets by using a conventional mechanical contact bending system together with a high-power diode laser source.

The obtained results can be summarized as follows.

1. The laser treatment during the forming process largely reduces the amount of energy released after the forming pressure is removed, and so counteracts the negative effect of the springback.
2. By combined experimental and statistical considerations (ANOM and ANOVA), a useful map of the most fruitful treatment conditions can be deduced.
3. A large energy input delivered towards the metal sheets contributes to minimizing the extent of springback of the pre-bent sheets provided that the material surface is neither damaged nor altered by too much heat.
4. The springback is almost invariant with the starting deflection, all other process conditions being kept constant.

These results illustrate the significant potential of the proposed hybrid forming technique.

A first-approximation regression equation and neural network solutions were used to model the hybrid forming process. The ability of different neural network models to predict the size of the springback was compared, and it was found that an MLP provides the best fit. The reliability of the best neural network solutions was checked by comparing it with the available experimental results as well as with an *ad hoc* analytical model. The MLP neural network trained by a BP algorithm was found to be a highly reliable modelling solution and very useful in simulation of process control and automation. Consequently, the basis for developing more sophisticated simulation tools to evaluate the hybrid forming process have been laid.

ACKNOWLEDGEMENTS

The authors would like to acknowledge Mr. Daniele Ceccarelli for his suggestions and stimulating insights during the development of the experimental plan of this paper and Prof. Vincenzo Tagliaferri for financing this work. Lastly, Clive Prestt kindly checked the English of this manuscript.

REFERENCES

1 **Dieter, G. E.** *Mechanical metallurgy*, third edition, 1998 (McGraw-Hill, London).
2 **Narasimhan, N.** and **Lovell, M.** Predicting springback in sheet metal forming: an explicit to implicit sequential solution procedure. *Finite Elem. in Anal. and Des.*, 1999, **33**, 29–42.
3 **Lan, F., Chen, J.,** and **Lin, J.** A method of constructing smooth tool surfaces for FE prediction of springback in sheet metal forming. *J. Mater. Process. Technol.*, 2006, **177**, 382–385.
4 **Cho, J. R., Moon, S. J., Moon, Y. H.,** and **Kang, S. S.** Finite element investigation on spring-back characteristics in sheet metal U-bending process. *J. Mater. Process. Technol.*, 2003, **141**(1), 109–116.
5 **Geng, L. M.** and **Wagoner, R. H.** Role of plastic anisotropy and its evolution on springback. *Int. J. Mech. Sci.*, 2002, **44**, 123–148.
6 **Li, K. P., Carden, W. P.,** and **Wagoner, R. H.** Simulation of springback. *Int. J. Mech. Sci.*, 2002, **44**, 103–122.
7 **Liu, Y. C.** The effect of restraining force on shape deviation in flanged channels. *ASME J. Engng Mater. Technol.*, 1988, **110**, 389.
8 **Sunseri, M., Cao, J., Karafillis, A. P.,** and **Boyce, M. C.** Accommodation of springback error in channel forming using active binder force control: numerical simulations and experiments. *ASME J. Engng Mater. Technol.*, 1996, **118**, 426.
9 **Moon, Y. H., Kang, S. S., Cho, J. R.,** and **Kim, T. G.** Effect of tool temperature on the reduction of the springback of aluminium sheets. *J. Mater. Process. Technol.*, 2003, **132**, 365–368.
10 **Shi, Y., Yao, Z., Shen, H.,** and **Hu, J.** Research on the mechanisms of laser forming for the metal plate. *Int. J. Mach. Tools Mf.*, 2006, **46**, 1689–1697.
11 **Costa Santos, E., Shiomi, M., Osakada, K.,** and **Laoui, T.** Rapid manufacturing of metal components by laser forming. *Int. J. Mach. Tools Mf.*, 2006, **46**, 1459–1468.
12 **Shen, H., Shi, Y., Yao, Z.,** and **Hu, J.** An analytical model for estimating deformation in laser forming. *Comput. Mater. Sci.*, 2006, **37**, 593–598.
13 **Barletta, M., Casamichele, L.,** and **Tagliaferri, V.** Line bending of Al_2O_3 coated and uncoated aluminium thin sheets. *Surf. Coat. Technol.*, 2006, **201**(3–4), 660–673.
14 **Geiger, M., Merklein, M.,** and **Pitz, M.** Laser and forming technology—an idea and the way of implementation. *J. Mater. Process. Technol.*, 2004, **151**(1/3), 3–11.
15 **Schuöcker, D.** Mathematical modeling of laser-assisted deep drawing. *J. Mater. Process. Technol.*, 2001, **115**(1), 104–107.
16 **Montgomery, D. C.** *Controllo Statistico della qualità*, 2006 (McGraw Hill, Milan).
17 **Liu, W., Liu, Q., Ruan, F., Liang, Z.,** and **Qiu, H.** Springback prediction for sheet metal forming based on GA-ANN technology. *J. Mater. Process. Technol.*, 2007, **12**, 227–231.
18 **Ko, D.-C., Kim, D.-H.,** and **Kim, B.-M.** Application of artificial neural network and Taguchi method to preform design in metal forming considering workability. *Int. J. Mach. Tools Mf.*, 1999, **39**, 771–785.
19 **Cheng, P. J.** and **Lin, S. C.** Using neural networks to predict bending angle of sheet metal formed by laser. *Int. J. Mach. Tools Mf.*, 2000, **40**, 1185–1197.
20 **Jeng-Jeng, J.-Y., Maub, T.-F.,** and **Leuc, S.-M.** Prediction of laser butt joint welding parameters using back propagation and learning vector quantization networks. *J. Mater. Process. Technol.*, 2000, **99**, 207–218.